December 1999 • NREL/SR-520-27665

Subcontractor Report

Electroabsorption and Transport Measurements and Modeling Research in Amorphous Silicon Based Solar Cells

Phase I Technical Progress Report March 24, 1998 — March 23, 1999

E.A. Schiff, J. Lyou, N. Kopidakis, P. Rao, and Q. Yuan
Department of Physics
Syracuse University
Syracuse, New York

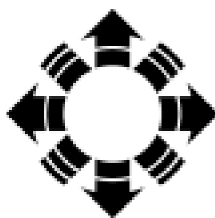

NREL
National Renewable Energy Laboratory
1617 Cole Boulevard
Golden, Colorado 80401-3393

NREL is a U.S. Department of Energy Laboratory
Operated by Midwest Research Institute • Battelle • Bechtel

Contract No. DE-AC36-99-GO10337

December 1999 • NREL/SR-520-27665

Electroabsorption and Transport Measurements and Modeling Research in Amorphous Silicon Based Solar Cells

Phase I Technical Progress Report March 24, 1998 — March 23, 1999

E.A. Schiff, J. Lyou, N. Kopidakis, P. Rao, and Q. Yuan
Department of Physics
Syracuse University
Syracuse, New York

NREL Technical Monitor: B. von Roedern

Prepared under Subcontract No. XAK-8-17619-23

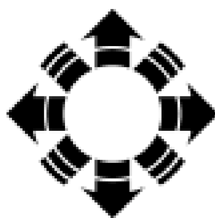

National Renewable Energy Laboratory

1617 Cole Boulevard
Golden, Colorado 80401-3393

NREL is a U.S. Department of Energy Laboratory
Operated by Midwest Research Institute • Battelle • Bechtel

Contract No. DE-AC36-99-GO10337

NOTICE

This report was prepared as an account of work sponsored by an agency of the United States government. Neither the United States government nor any agency thereof, nor any of their employees, makes any warranty, express or implied, or assumes any legal liability or responsibility for the accuracy, completeness, or usefulness of any information, apparatus, product, or process disclosed, or represents that its use would not infringe privately owned rights. Reference herein to any specific commercial product, process, or service by trade name, trademark, manufacturer, or otherwise does not necessarily constitute or imply its endorsement, recommendation, or favoring by the United States government or any agency thereof. The views and opinions of authors expressed herein do not necessarily state or reflect those of the United States government or any agency thereof.

Available electronically at http://www.doe.gov/bridge

Available for a processing fee to U.S. Department of Energy
and its contractors, in paper, from:
U.S. Department of Energy
Office of Scientific and Technical Information
P.O. Box 62
Oak Ridge, TN 37831-0062
phone: 865.576.8401
fax: 865.576.5728
email: reports@adonis.osti.gov

Available for sale to the public, in paper, from:
U.S. Department of Commerce
National Technical Information Service
5285 Port Royal Road
Springfield, VA 22161
phone: 800.553.6847
fax: 703.605.6900
email: orders@ntis.fedworld.gov
online ordering: http://www.ntis.gov/ordering.htm

Printed on paper containing at least 50% wastepaper, including 20% postconsumer waste

Introduction

Preface

This research project has two broad objectives:

- We seek a deeper understanding of the open circuit voltage V_{OC} in amorphous silicon based solar cells, and in particular we wish to determine whether the present open-circuit voltages in these cells can be increased. We combine experimental studies of device operation with solar cell modeling.
- We seek to measure and to understand electron and hole photocarrier drift under electric fields for the technologically significant forms of amorphous-silicon based materials. We incorporate this knowledge into solar cell device models in an effort to deepen our understanding of solar cell operation.

In addition to the support from the National Renewable Energy Laboratory, this research received support from the Korea Research Foundation and from Korea University for Prof. Lyou's research leave at Syracuse University.

Summary

In Phase I of this project we have done significant work on the following topics:

1. *Electroabsorption measurements and built-in potentials in a-Si:H based solar cells and devices.* We have worked on two projects. The more successful has been estimates of V_{bi} in cells with a-SiGe:H absorber layers from United Solar Systems Corp.; this work is in collaboration with Jeff Yang and Subhendu Guha. We obtain an estimate of V_{bi} = 1.17 V in these cells which is quite convincing. Additionally we have done extensive measurements on a series of TCO/i/n diodes from Institute for Energy Conversion at University of Delaware. This work was in collaboration with Steven Hegedus. Estimates of V_{bi} in these structures were not conclusive and will not be included here.
2. *Solar cell modeling employing the AMPS computer program.* We have been successful in installing and using the PC version of the AMPS modeling program written by Steve Fonash's group at Penn State. We have begun operating a simple "AMPS" modeling site (http://physics.syr.edu/~schiff/AMPS). In our modeling research in Phase I, we have explored the effect of conduction bandtail width upon V_{oc} computed analytical approximations and the AMPS program. There are quantitative differences between the two procedures which we discuss. We have uncovered a V_{oc} saturation effect in AMPS modeling which we have not yet explained.
3. *Drift-mobility measurements in a-Si:H made with high hydrogen dilution.* We have measured electron and hole mobilities in several *n/i/m* cells from Pennsylvania State University with a-Si absorber layers made under maximal hydrogen dilution; this work is in collaboration with Zhou Lu and Chris Wronski at Penn State. We find a modest *increase* in hole mobility in these materials compared to conventional a-Si:H.
4. *Electroabsorption spectroscopy in solar cells.* An unexpected byproduct of our work estimating V_{bi} has been discovery and interpretation of an infrared absorption band near 1.0 eV. We believe that this band is due to dopants & defects at the *n/i* interface of the cells. The existence of the band also has interesting implications for the nature of electroabsorption and for the doping mechanism in *n*-type material. Collaborators in this work include the Steven Hegedus (Institute of Energy Conversion, Univ. of Delaware), Rafik Middya (Solarex Thin Films Division), Jeff Yang and Subhendu Guha (United Solar Systems Corp.)

Table of Contents

Preface 1
Summary 1
Table of Contents 2
Table of Figures 3
Electroabsorption measurements and built-in potentials 4
Introduction 4
Samples and Spectroscopic Details 4
Built-in Potential Estimates 6
Discussion 7
References 8
Computer Modeling Studies 9
Modeling Web Site 9
Tests of AMPS vs. Tiedje's Model 9
Effect of Conduction Bandtail Broadening Upon V_{OC} 11
Drift Mobilities in a-Si:H Made at Maximal Hydrogen Dilution 12
References 14
Sub-bandgap interfacial electroabsorption in amorphous silicon 15
Introduction 15
Experimental Information 16
Electromodulation Measurements 16
Models for Sub-Bandgap Electromodulation 18
References 21

Table of Figures

Fig. 1: Electromodulated reflectance spectra for four *nip* a-SiGe and a-Si based solar cells with varying absorber layer bandgaps. The "unprocessed" spectrum illustrates the large interference fringes resulting from superposition of back-surface reflected light with light directly reflected from the top layers of the cell. The remaining spectra are the upper envelopes of the unprocessed spectra. 5

Fig. 2: Electromodulated reflectance signal $\delta R/(R\delta E)$ as a function of the external electrostatic potential across the cell. Measurements are shown for several wavelengths along with linear regression lines. 6

Fig. 3: Wavelength dependence of the electroabsorption offset potential V_0 for four *pin* solar cells (prepared at USSC) with a-SiGe:H absorber layers of differing thicknesses; the typical optical gap was 1.5 eV. The long wavelength limit of about 1.17 V is an estimate of the built-in potential; open-circuit voltages ranged from 0.65 - 0.79 V under AM1 conditions. Sample codes (by thickness): (0.25 μm, LINE 10024) (0.50 μm, LINE 10239) (1.0 μm, L8702) (1.5 μm, L8692). 7

Fig. 4: Comparison of open-circuit Voltages V_{oc} calculated using AMPS PC-1D and Tiedje's analytical approximation. The conduction bandtail width was varied as indicated; the other modeling parameters are described in the text. A uniform photogeneration rate 1.1 x 10^{21} $cm^{-3}s^{-1}$ was used. 9

Fig. 5: AMPS calculations of spatial variation of the valence bandedge and the hole quasi-Fermi level for uniform photogeneration (1.1 x 10^{21} $cm^{-3}s^{-1}$) and open-circuit conditions. The calculations are associated with the open-circuit Voltages of Fig. 4 for four conduction bandtail widths; from the lowest to the uppermost curves, the widths were 20, 30, 40, and 50 meV. The p-layer extends to 20 nm, and the n-layer starts at 520 nm.The electron quasi-Fermi-level is at 0.0 V throughout the intrinsic layer and n-layers. 10

Fig. 6: Hole photocurrent transients for three fields measured in sample CW 81at 250 K using a 450 nm laser pulse.12

Fig. 7: Temperature-dependent hole drift mobilities for three samples of a-Si:H made with "maximal" hydrogen dilution. 13

Fig. 8: Hole drift mobilities at 293 K for several varieties of a-Si:H. MD refers to "maximal dilution" samples prepared at Pennsylvania State University. Hot-wire refers to a prior report of mobilities in a hot-wire sample prepared at NREL. All mobilities refer to a displacement/field ratio $L/E = 2 \times 10^{-9}$ cm^2/V. 14

Fig. 9: The two panels show the electromodulated reflection spectra for a-Si:H based *nip* diodes from United Solar Systems Corp. The upper panel illustrates the dependence upon the amplitude of the electric field modulation assuming a uniform field across the undoped intrinsic layer. Both the sub-bandgap and interband electromodulation is essentially linear in electric field. The lower panel illustrates the dependence upon the mean, unmodulated external electric field across the diode; the sub-bandgap electromodulation is independent of the unmodulated field, whereas the interband electromodulation depends linearly upon it. 17

Fig. 10 Normalized electromodulated transmittance $\delta T/(T\delta E)$ for two Schottky diodes from the Institute of Energy Conversion amorphous silicon {IEC (a)} and microcrystalline silicon {IEC (μ)} n^+ layers, and for one *pin* solar cell from Solarex Thin Films Division (SLX). For each sample results for several DC biases are presented; from the topmost curve of each family the mean fields were (IEC(a) - 1.5, 4.5, and 3.6×10^6 V/m, IEC (μ) - 13.4, 7.6, and 3.6×10^6 V/m, SLX 10.0 and 20.0×10^6 V/m). 18

Fig. 11: Schematic illustrating the optical transitions in an *n*-type a-Si:H layer involved in the model proposed for reverse-bias electromodulation; note in particular the 0.8 eV transition from the well-localized D^- (negatively charged dangling bond) center to a nearby, relatively extended bandtail state, as well as the unidentified 1.1 eV transition. 19

Electroabsorption measurements and built-in potentials

Introduction

The built-in potential V_{bi} across a solar cell is among its most important device parameters. For amorphous silicon-based solar cells, there is at best only a semi-quantitative knowledge of V_{bi}. The two most promising approaches for estimating V_{bi} are *electroabsorption* measurements,[1] which infer V_{bi} from the dependence of optical absorption upon electric-field, and *low-temperature saturation* of the open-circuit voltage V_{oc}, which may be identifiable with V_{bi}.[2] Neither method has proved to be ideal in previous work. The interpretation of electroabsorption depends upon the distribution of the internal electric field between the intrinsic and p^+ layers of a cell, which greatly complicates estimation of V_{bi}. The low-temperature saturation method of course depends upon a particular assumption about the electrical properties of a cell at low temperatures which is also difficult to justify conclusively.

Most prior work on V_{bi} has emphasized amorphous-silicon solar cells with “standard” a-Si:H absorbers (optical gaps about 1.75 eV). In the present work we present electroabsorption measurements on cells with narrow bandgap absorbers based on a-SiGe:H alloys. This work is of course a potentially useful extension of the earlier measurements, since there is (to our knowledge) no experimental information on V_{bi} in cells incorporating a-SiGe. Perhaps equally important, our results indicate that electroabsorption measurements in solar cells with a-SiGe:H absorber layers largely avoid the interpretive difficulties associated with cells with a-Si:H absorbers. For the latter, the p^+ and intrinsic layers have comparable, but quantitatively different, electroabsorption spectra. This complicates estimation of V_{bi}. For cells with a-SiGe:H absorber layers, the electroabsorption signal is much more completely dominated by the behavior of the a-SiGe:H absorber layer, leading to a more direct estimate for V_{bi}.

We find for a series of cells with varying a-SiGe:H absorber layer thicknesses that V_{bi} = 1.17 V. This value is substantially larger than the typical open-circuit voltages (0.7 V) measured under solar illumination in these cells. It suggests that V_{bi} is not a substantial limitation to V_{oc} for cells with "narrow gap" absorbers.

Samples and Spectroscopic Details

UNI-SOLAR Code	*Thickness* (nm)	V_{oc} (V)	*FF*	*Optical Gap* (eV) (nominal)
LINE 10012 #22	220	0.955	0.705	1.7
LINE 10011 #32	150	0.794	0.63	1.55
LINE 10009 #33	150	0.699	0.558	1.50
LINE 10024 #22	140	0.65	0.549	1.45
LINE 10239	280	0.700	0.488	1.50
L 8692	1500	-	-	1.50
L 8693	1500	-	-	1.50
L 8702	1000	-	-	1.50

Table 1: Properties of eight Uni-Solar samples used in the present study. All of these cells have the structure ss/n^+/*i*/p^+/TCO (ss: stainless steel, TCO: transparent conductive oxide); n^+ layers are a-Si:H:P, p^+ layers are μc-Si:H:B.

The present work was done on two series of a-Si:H based *nip* solar cells prepared at United Solar Systems Corp.. Sample information is summarized in Table 1. The substrate material for these cells is stainless steel. All cells used comparable a-Si:H n^+ and μc-Si:H p^+ layers; samples varied in the thickness and bandgaps of the intrinsic absorber layers. For all but one of the samples, the absorber layer was based on a-SiGe:H alloys; one sample used unalloyed a-Si:H.

The actual measurement performed on these cells was electroreflectance. We used a beam from a monochromator to illuminate the specimen; the light reflected from top contact of the sample was detected using either a Si or an InGaAs diode detector. The reflectance was modulated by the reverse bias voltage across the cell. Since these cells have a top, anti-reflection coating, relatively little of the illumination is reflected from the first interfaces. For longer wavelengths, most of the illumination travels across the absorber layer. A substantial fraction (we estimate about 0.4) is reflected at the back stainless-steel contact. This back-surface reflected light travels back up through the absorber layer and exits the sample, following a path similar to that of directly reflected light. The Osaka University group, which did the pioneering work on V_{bi} estimation using electroabsorption,[3] dubbed this detection arrangement as "back surfaced reflected electroabsorption" (BASREA), since the intensity of the back-surface reflected beam is modulated by electric-fields through the electroabsorption effect. Of course the amplitude of the back-surface reflected beam interferes with the directly reflected beam, which may complicate optical analysis in some cases.

Electromodulated reflectance spectra $\delta R/(R\delta E)$ measured for the four thinnest cells are presented in Fig. 1. δE is the amplitude of the field modulation across the cell's absorber layer; all spectra were measured

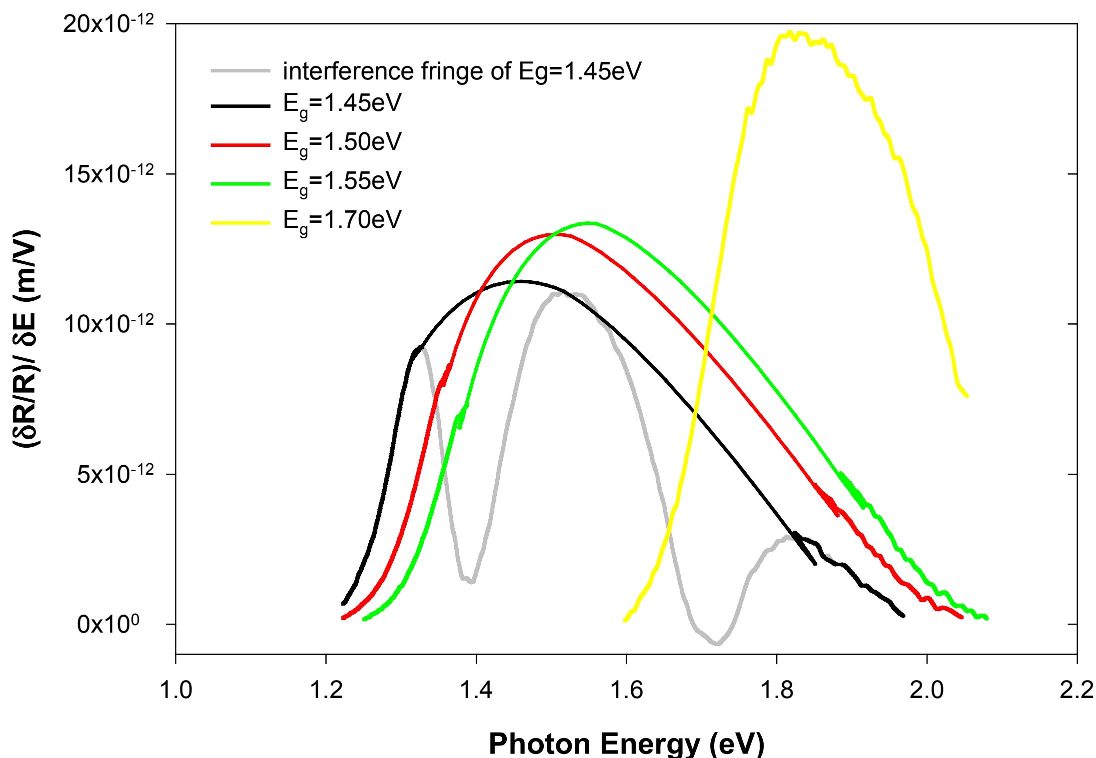

Fig. 1: Electromodulated reflectance spectra for four *nip* a-SiGe:H and a-Si based solar cells with varying absorber layer bandgaps. The "unprocessed" spectrum illustrates the large interference fringes resulting from superposition of back-surface reflected light with light directly reflected from the top layers of the cell. The remaining spectra are the upper envelopes of the unprocessed spectra.

under 2 V reverse bias. One of the spectra is "unprocessed" and shows the extent of the interference fringes. The remaining spectra are the upper envelopes of the fringes, one of which corresponds to the unprocessed spectrum. Despite the ambiguities associated with the fringes, it is fairly evident that the peak of the spectra track the bandgaps of the absorber layers in the cells fairly well. The strengths of the electroabsorption spectra scale with the absorber layer thickness fairly well.

Built-in Potential Estimates

The essential measurement from which we estimate built-in potentials is the dependence of the electromodulation signal upon the DC potential drop V across the cell. Electroabsorption is quadratic with electric field in a-Si:H. Electromodulation essentially measures a derivative of the field-dependence, leading to the linear dependence upon V. We illustrate measurements for one sample in Fig. 2. The slope of the regression lines indicates the strength of the electroabsorption; the voltage-axis intercept V_0 is related to the built-in potential V_{bi} across the cell. The wavelengths selected for these measurements are those corresponding to maxima in the electromodulated reflection signal.

As is evident from Fig. 2, there is some dependence of V_0 upon photon energy. This dependence precludes an immediate idenification of V_0 with V_{bi}. For the present measurements, it appears that a fairly simple effect is responsible. In Fig. 3 we illustrate the spectrum of V_0 for four samples with similar bandgaps and varying thicknesses. For the three thicker samples there is a common low energy limit of about 1.17 V. We believe that this value can be interpreted as V_{bi} for these cells. The thinnest sample, which also had a slightly lower bandgap, has a slightly smaller value in this limit.

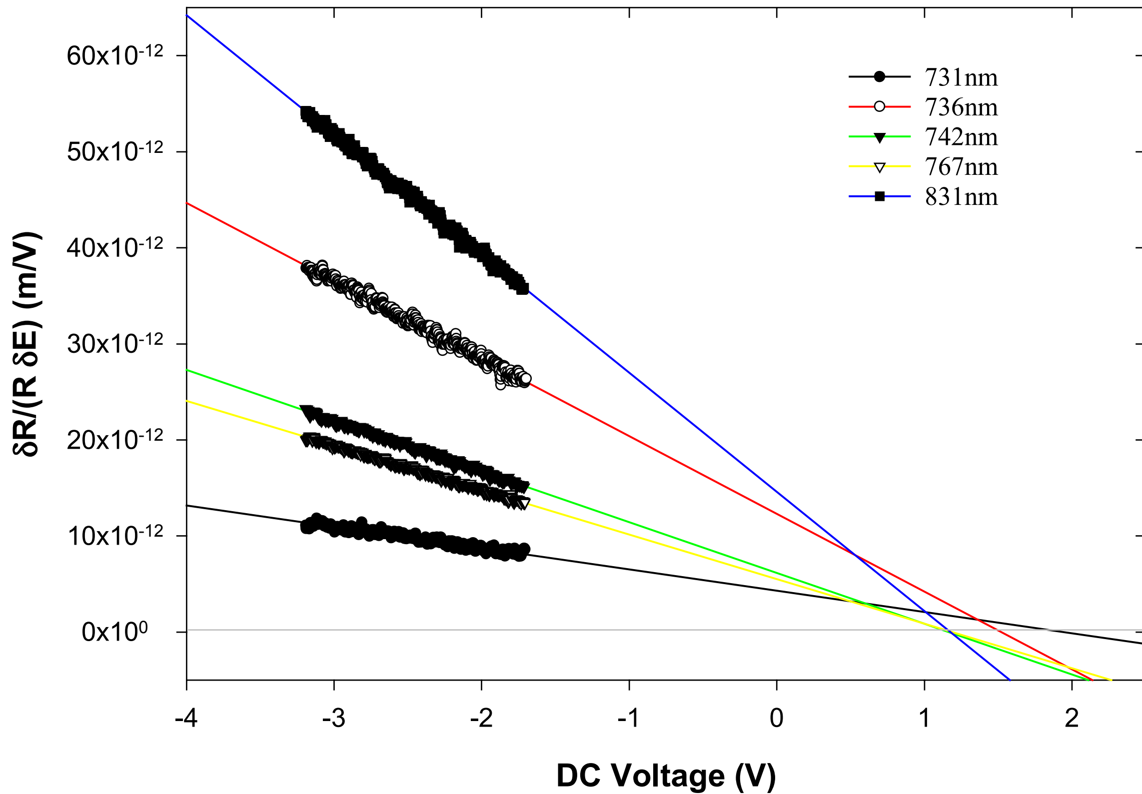

Fig. 2: Electromodulated reflectance signal $\delta R/(R\delta E)$ as a function of the external electrostatic potential across the cell for sample code L8702. Measurements are shown for several wavelengths along with linear regression lines.

For all four samples there is a transition to a substantially larger value for V_0 at shorter wavelengths. The thickness-dependence of the transition suggests that this effect is due to the change in the spatial origin of the electromodulation signal. For longer wavelengths the signal is sensitive to back-surface reflection of the incident light: interband optical absorption is fairly negligible. For shorter wavelengths interband absorption becomes much stronger, and the electromodulation signal is dominated by light reflected at the top of the cell. Indeed it is possible that the signal in this short-wavelength limit is dominated by the electroabsorption effect of the p^+ layer, since at the shorter wavelengths the electroabsorption strength is larger in the wider bandgap p^+ material than in the narrower bandgap intrinsic material. The most satisfactory view we have found is that this short-wavelength value for V_0 indicates the scaling of the field at the *p/i* interface. The numerical value for V_0 may be useful as a constraint on model calculations, but otherwise does not appear to be directly interpretable.

Discussion

The value V_{bi} = 1.17 V we propose for cells with narrow bandgap (1.50 eV) absorbers is larger than the value $V_{bi} \approx 1.05$ V which we have previously inferred for otherwise comparable cells with "ordinary" (1.75 eV) a-Si:H absorbers.[1] It is somewhat smaller than our estimate $V_{bi} \approx 1.25$ V for cells with a-Si:H absorbers made with high hydrogen dilution.We have somewhat more confidence in the present measurements, for which we have not applied any corrections for the competition of the electroabsorption in the p^+ and intrinsic layers: there is relatively little overlap between electroabsorption bands for a narrow bandgap intrinsic layer and a microcrystalline *p*-layer.

This variability is at least mildly surprising. Since the *n* and *p* layers of all of these cells are made with essentially the same recipes, and since one's first estimate for V_{bi} is simply the difference between the Fermi levels in these two doped layers, one might expect no variation due to changes in the the intrinsic layer separating the two doped layers. We have previously suggested that interface dipole effects reduce the built-in potential below the value which would be inferred from the properties of free-standing n^+ and

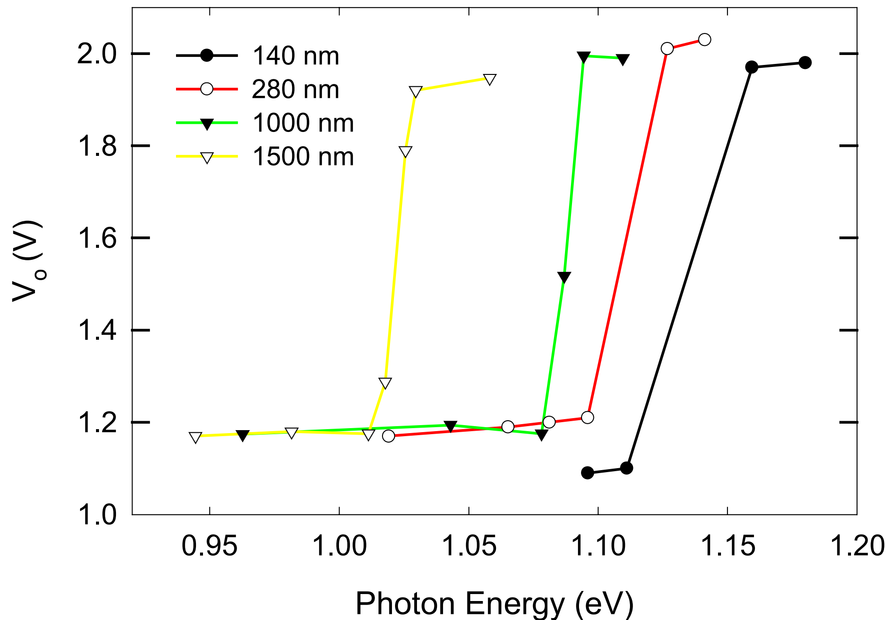

Fig. 3: Spectrum of the electroabsorption offset potential V_0 for four *nip* solar cells (prepared at USSC) with a-SiGe:H absorber layers of differing thicknesses; the typical optical gap was 1.5 eV. The low energy limit of about 1.17 V is an estimate of the built-in potential; open-circuit voltages ranged from 0.65 - 0.70 V under AM1 conditions. Sample codes (by thickness): (140 nm, L10024) (280 nm, L10239) (1000 nm, L8702) (1500 nm, L8692).

p^+ layers. We still consider this entirely plausible; in addition to the electroabsorption measurements, there are several estimates of interfacial band offsets which, in our estimation, suggest interface dipole effects. Nonetheless it is only fair to note two difficulties. First, there is no obvious logic to the variability of V_{bi} for cells with varying absorbers. Second, the Urbana-Champaign group has failed to detect significant dipole formation in Kelvin probe studies of interfaces between doped and intrinsic layers formed using magnetron sputtering.[4]

References

[1] Lin Jiang, Qi Wang, E. A. Schiff, S. Guha, J. Yang, Xunming Deng, *Appl. Phys. Lett.* **69**, 3063 (1996).

[2] C. R. Wronski, R. W. Collins, J. S. Burnham, I.-S. Chen, H. Fujiwara, L. Jiao, Y. Lee, Z. Lu, S. Kim, A. Ferlauto, J. Koh, H. Liu, X. Niu, and S. Semoushkina, *Wide Band Gap Solar Cells with High Stabilized Performance* (Final Subcontract Report to the National Renewable Energy Laboratory, 15 July 1994 – 15 March 1998, NREL/SR-520-25271), p. 110.

[3] S. Nonomura, H. Okamoto, and Y. Hamakawa, *Appl. Phys. A* 32, 31 (1983).

[4] A. Nuruddin and J. R. Abelson, *Appl. Phys. Lett.* **71**, 2797 (1997).

Computer Modeling Studies

Modeling Web Site

We have created a web-site to support a-Si:H solar cell modeling research: http://physics.syr.edu/~schiff/AMPS. This web-site contains three main types of information:

1. A *journal* containing comments based on our experience with AMPS PC-1D.
2. *AMPS parameter files* used in our research, along with discussions of the parameter choices. In this report, we refer the reader to these web-pages for further discussions of parameters used in our research.
3. A *calculator* implementing Tiedje's approximate calculation of the open-circuit voltage for amorphous semiconductor solar cells.

The web-site is intended to complement the web-site http://www.psu.edu/dept/AMPS maintained by Steve Fonash's research group at Penn State University, which developed the AMPS modeling programs.

Tests of AMPS vs. Tiedje's Model

One major objective of our research is to develop a better understanding of the open-circuit voltage in amorphous silicon based solar cells. Certainly the simplest picture for V_{oc} in amorphous semiconductors is that proposed in 1982 by Tom Tiedje. Tiedje suggested that the fundamental exponential bandtails in amorphous semiconductors would represent the ultimate limit to open-circuit voltages in working cells. He neglected other defects, and developed a relatively simple calculation for V_{oc} based on quasi-Fermi level positions in the bulk semiconductor under illumination. Tiedje's work now seems remarkably prescient: the open-circuit in amorphous-silicon based solar cells is relatively independent of defect densities.

As an initial project, we chose to make a comparison of open-circuit voltages calculated using Tiedje's

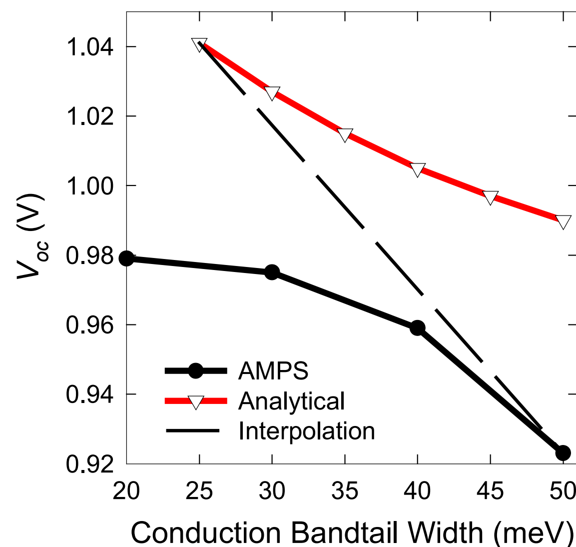

Fig. 4: Comparison of open-circuit Voltages V_{oc} calculated using AMPS PC-1D and Tiedje's analytical approximation. The conduction bandtail width was varied as indicated; the other modeling parameters are described in the text. A uniform photogeneration rate 1.1 x 10^{21} $cm^{-3}s^{-1}$ was used.

approximation and AMPS PC-1D. We have experimented with several sets of parameters. In this report we compare calculations using a set of intrinsic layer parameters devised to be consistent with electron and hole drift-mobility measurements. The parameter set does not include any deep levels in the intrinsic layer. Doped layer and contact parameters are largely taken from the set "pin_a-Si.AMP" included with the PC-1D AMPS version distribution set; the p-layer of this set is intended to model a-SiC:H:B p-layers, and the n-layer models a-Si:H:P. The valence bandtail width was set to 50 meV and the mobility-gap was set to 1.80 eV. Further discussion of these parameters may be found on the web at http://physics.syr.edu/~schiff/AMPS/SU_Parameter_Suggestions.html.

We chose to explore varying the conduction bandtail width upon the open-circuit voltage; this exercise should help decide how much the increasing conduction bandtail width in a-SiGe:H alloys affects open-circuit Voltages in narrow bandgap cells. A comparison of the AMPS and the analytical calculation is presented as Fig. 4 for cells with a 500 nm thick intrinsic layer and a constant volume generation rate of about 1.1×10^{21} $cm^{-3}s^{-1}$; the conduction bandtail widths were varied from 20 meV to 50 meV as shown. The corresponding spatial profiles for the hole quasi-Fermi level and for the valence bandedge from the AMPS PC-1D calculations are presented in Fig. 5; to read these profiles one must know that the electron quasi-Fermi-level is located at 0.0 eV throughout the intrinsic and n-type layers.

These calculations raise several issues. We defer discussion of the quantitative discrepancy between the analytical and AMPS calculations, and instead commence with a discussion of the AMPS open-circuit Voltages and the associated profiles. The electron quasi-Fermi-level E_{fn} is not shown, but was constant at 0.0 eV across the intrinsic and n-layers. A constant E_{fn} is one's first expectation for results at open-circuit Voltage, since it suggests that electron currents are negligible. Similarly, the hole quasi-Fermi-levels E_{fp} are essentially constant for the 30, 40, and 50 meV widths. For these bandtail widths the open-circuit Voltage computed by AMPS PC-1D does agree well with the level of E_{fp}, in agreement with the assumption of the analytical calculation equating $V_{oc} = E_{fn}-E_{fp}$.

A close examination of the hole quasi-Fermi level for a 20 meV conduction bandtail width in Fig. 4

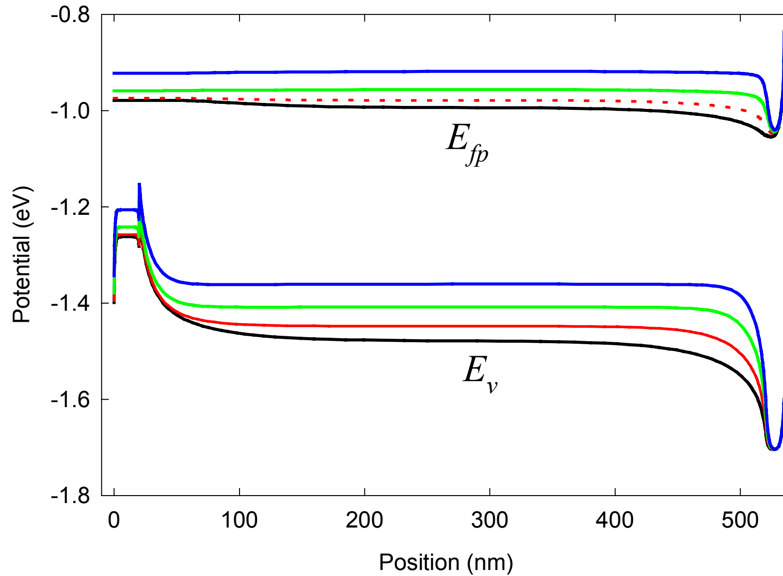

Fig. 5: AMPS calculations of spatial variation of the valence bandedge and the hole quasi-Fermi level for uniform photogeneration (1.1 x 10^{21} $cm^{-3}s^{-1}$) and open-circuit conditions. The calculations are associated with the open-circuit Voltages of Fig. 4 for four conduction bandtail widths; from the lowest to the uppermost curves, the widths were 20, 30, 40, and 50 meV. The p-layer extends to 20 nm, and the n-layer starts at 520 nm.The electron quasi-Fermi-level is at 0.0 V throughout the intrinsic layer and n-layers.

shows a distinct spatial variation near the *p/i* interface. It is this effect which causes the "saturation" of V_{oc} for smaller bandtail widths in Fig. 5: V_{oc} may be equated for these simulations with the value for E_{fp} *in the p-layer*, so the fall of E_{fp} to lower values in the *i*-layer is not reflected. What surprises us is that this effect sets in at much lower values for V_{oc} than V_{bi}, which was near 1.6 V for this calculation. We have not yet understood this effect.

Effect of Conduction Bandtail Broadening Upon V_{OC}

We now return to the quantitative comparison of the analytical and AMPS calculations for V_{oc}. The analytical calculation is probably not very accurate for larger conduction bandtail widths (45 - 50 meV) since the calculation exploits the assumption that the conduction bandtail is distinctly narrower than the valence bandtail. Similarly, the saturation of V_{oc} for smaller conduction bandtail widths in the AMPS simulation represents some sort of contact effect which we don't understand; it is likely that the analytical calculation may give a better estimate of the limit to V_{oc} due only to the intrinsic layer. We speculate that the straight line interpolating between the two calculations may represent the "true" limit to V_{oc} set by the intrinsic layer.

If we accept this interpolation, we can conclude that V_{oc} declines by approximately $\Delta E_{0,c}/2e$ as the conduction bandtail width $E_{0,c}$ is increased. Amorphous silicon-based solar cells have been studied with absorber-layer bandgaps E_G from (roughly) 1.85 eV to 1.45 eV; remarkably, the variation in V_{oc} is essentially the same as that of E_G/e, falling from 1.05 to 0.65 V over this same range of absorber layer gaps. This 1:1 variation is very surprising, since both the defect density and the conduction bandtail width $E_{0,c}$ are known to increase as bandgaps diminish. We can, however, now largely exclude the increase of $E_{0,c}$ as a significant effect. The present studies suggest only a diminishment by 0.015 V in V_{oc} due to a increase in $E_{0,c}$ from 20 meV to 50 meV, which is insignificant in comparison to the 0.4 V change in the gap energy.

Drift Mobilities in a-Si:H Made at Maximal Hydrogen Dilution

Thin-film silicons made using silane gas diluted with hydrogen have structures ranging from amorphous to microcrystalline; a transition occurs as the hydrogen dilution is increased.[1] Amorphous silicon layers made at the maximal dilution for which an amorphous structure is retained have several interesting properties. First, they tend to have slightly larger optical bandgaps than lower-dilution amorphous materials, which makes them potentially useful for preparing high V_{OC} cells. Second, there is some evidence that maximal-dilution materials have better stabilized electronic properties than low-dilution materials. These properties must of course be considered in the context of the lower deposition rates for layers as hydrogen dilution increases.

We have measured hole mobilities in three a-Si:H samples made at high dilution by Prof. Christopher Wronski's research group at Pennsylvania State University. The a-Si:H layers are deposited on SnO_2-coated glass (Corning 7059). The structure of the samples is glass/SnO_2/a-Si:H:P (n+)/a-Si:H (i)/Ni. The a-Si:H layers were deposited using a Tek-Vak MPS 4000-LS multi-chamber PECVD system. The intrinsic-layer deposition was done using a substrate temperature of 200 C and a hydrogen/silane ratio of 10:1. (200 C, R=H_2/SiH_4=10:1). The n+ layer was 35 nm thick and has an activation energy for electrical conduction of 0.25 eV. A top semi-transparent Schottky barrier was formed by thermal evaporation of Ni onto the intrinsic layer immediately following a short etching with buffered hydrofluoric acid; small, circular Ni electrodes of area 0.02 cm^2 were formed; the thickness of the Ni films was 15 nm. Three different samples were prepared over several months; the sample codes and their thicknesses are (CW81 - 1.1 microns, PSU 020299R – 1.5 microns, PSU 031599R - 1.47 microns).

In Fig. 6 we show hole photocurrent transients in sample CW81. The transients have the features

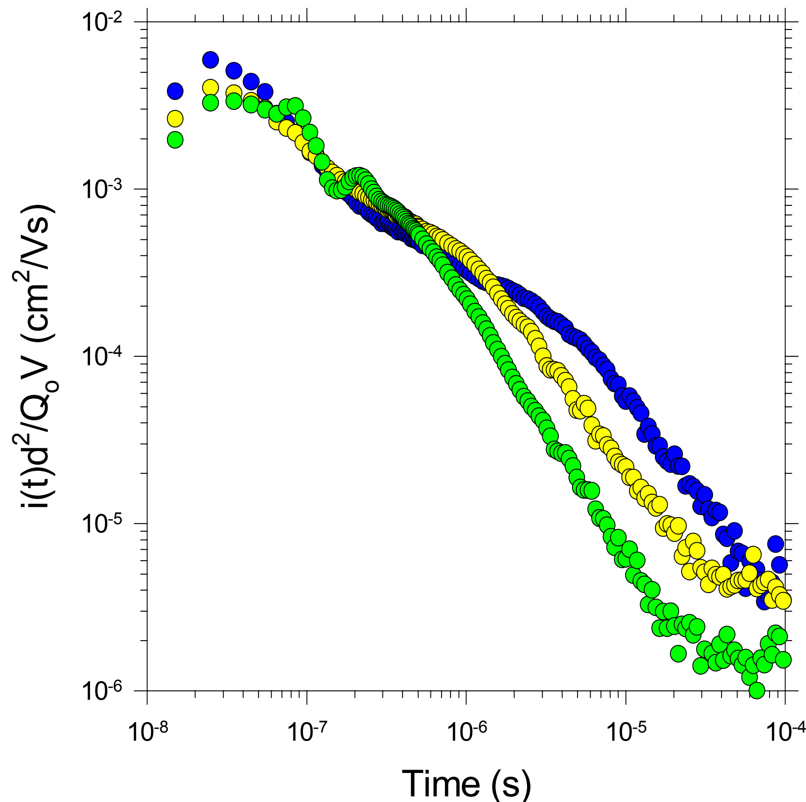

Fig. 6: Hole photocurrent transients for three fields measured in sample CW 81at 250 K using a 450 nm laser pulse.

required for extraction of drift-mobilities. At shorter times there is an "envelope" which is common for the several voltages; this is a consequence of linear or "Ohmic" transport of holes. Although not shown here, the total charge measured by integration of *i(t)* is essentially the same for each transient, so one is confident that the interpretation of the transients in terms of a drifting distribution of photogenerated holes is valid. At longer times transients have a steeper descent which is caused by hole sweepout. The corresponding transit times occur earlier for the higher field transients.

Transients such as these can be readily used to extract drift-mobilities characteristic of a specific ratio L/E of hole displacement L and field E; we usually use $L/E = 2 \times 10^{-9}$ cm^2/V for comparing differing materials. In Fig. 7 we show the temperature-dependence measured for three samples of H-diluted a-Si:H, along with a regression fit from hole measurements in conventional a-Si:H.[2] All samples are noticeably above the regression line, indicating improved values for the hydrogen-diluted samples.

In Fig. 8 we present a comparison of our mobility measurements at 293 K for a variety of species of a-Si:H. Note that all samples of maximal dilution a-Si:H measured to-date have enhanced hole mobilities (up to fivefold) compared to our measurements on conventional, low-dilution a-Si:H. We have previously reported a comparably large hole mobility in some hot-wire deposited a-Si:H.[3] On balance it now seems plain that improved hole mobilities are achievable in a-Si:H.

We have not yet made a serious effort to extract fitting parameters for the standard, exponential bandtail multiple-trapping model for the drift-mobilites in H-diluted a-Si:H. We presume that the bandtail width is

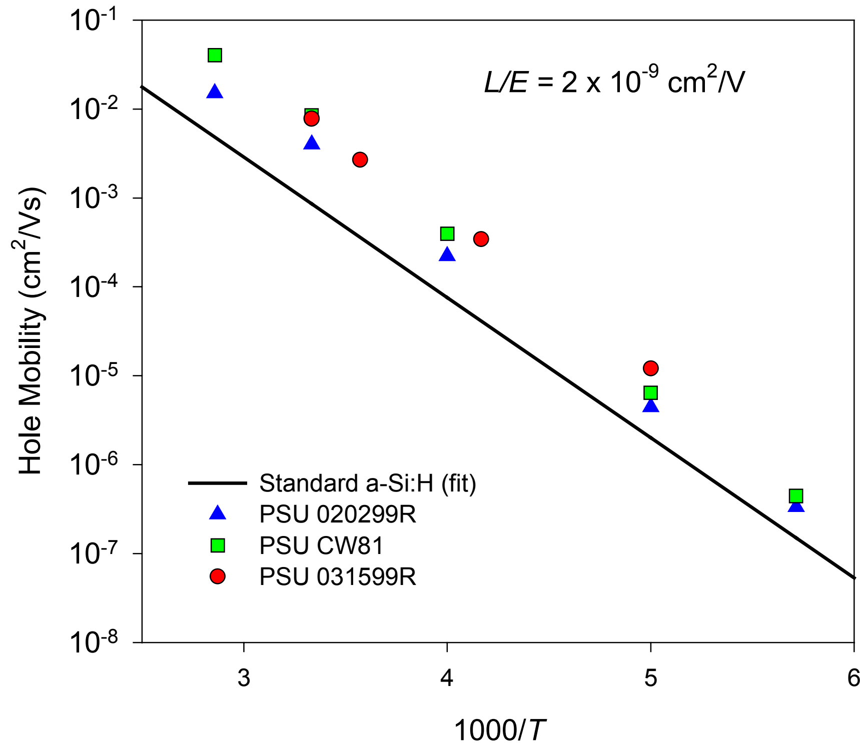

Fig. 7: Temperature-dependent hole drift mobilities for three samples of a-Si:H made with "maximal" hydrogen dilution.

slightly smaller for the hydrogen-diluted material.

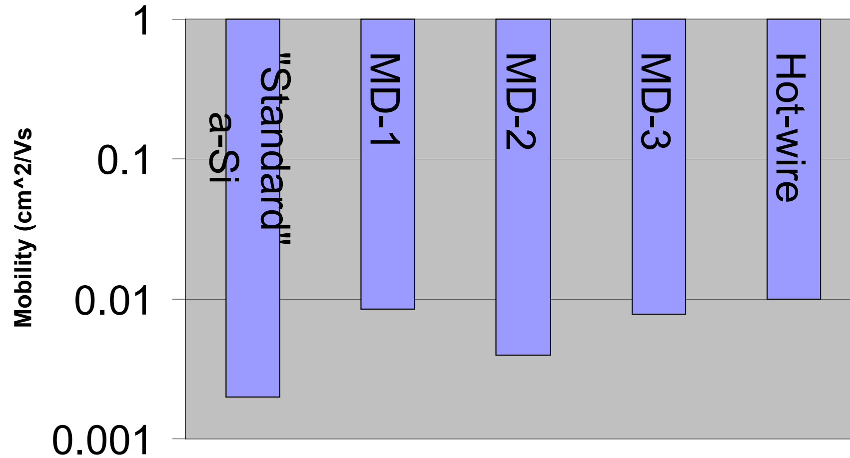

Fig. 8: Hole drift mobilities at 293 K for several varieties of a-Si:H. MD refers to "maximal dilution" samples prepared at Pennsylvania State University. Hot-wire refers to a prior report of mobilities in a hot-wire sample prepared at NREL.[3] All mobilities refer to a displacement/field ratio $L/E = 2 \times 10^{-9}$ cm^2/V.

References

[1] S. Guha, J. Yang, D. L. Williamson, Y. Lubianiker, J. D. Cohen, and A. H. Mahan, *Appl. Phys. Lett.* **74**, 1860 (1999).

[2] Q. Gu, Q. Wang, E. A. Schiff, Y.-M. Li, and C. T. Malone, *J. Appl. Phys.* **76**, 2310 (1994).

[3] E. A. Schiff, Q. gu, L. Jiang, J. Lyou, I. Nurdjaja, and P. Rao, *Research on High-Bandgap Materials and Amorphous Silicon-Based Solar Cells: Final Technical Report* (NREL document SR-520-25922, 1998), p. 31.

Sub-bandgap interfacial electroabsorption in amorphous silicon

We have measured the sub-bandgap electroabsorption spectra in several amorphous silicon *pin* and Schottky barrier diodes under reverse bias. While the spectra do vary, for several samples we find a sharp feature at 0.8eV and a less prominent band at 1.1 eV. We present a model for this electroabsorption based on optical transitions near the interface of the *n*-type and undoped layers of the diodes; an unusual feature is that the optical spectrum appears to be a direct map of the energy distribution of deep levels in the *n*-type material, as opposed to a convolution of defect and extended-state bands. We associate the 0.8 eV band with the D^- level (negatively charged dangling bond) based on previously published properties; we have not identified the defect responsible for the 1.1 eV feature. We use the method to compare interfaces between doped layers in one series of samples.

Introduction

Electroabsorption is the change in optical absorption due the application of a voltage bias across a sample. It is thus a form of modulation spectroscopy, and can offer insights not readily available from more direct optical measurements. Electroabsorption was first developed to study the band structure of crystalline solids. In amorphous semiconductors electroabsorption measurements corresponding to interband optical transitions indicate that electric fields warp the wavefunctions of nearly localized electronic states near mobility edges;[1] the effect is quadratic in the applied electric field. Investigators have explored the relationship between electroabsorption and the mobilities that govern photocarrier transport in the bands,[2] as well as the possibility of light-soaking effects on electronic states at the bandedges.[3]

There has been relatively little work done on electroabsorption corresponding to defect-related optical properties. The defect-related analog of the interband effect just described would be several orders of magnitude weaker, since the absorption coefficient for transitions involving mid-band gap states is far lower than the interband absorption, and would presumably share its quadratic dependence upon electric field. While this type of electroabsorption has not been observed, defect-related electromodulation was reported by Eggert and Paul[4] in forward-biased a-Si:H diodes. In this case, electric-field induced warping of electronic states is no longer responsible for the electromodulation, and the effect is not quadratic in electric field. Changes in defect occupancy in the intrinsic layer due to injection of space-charge by forward bias lead to the readily observable changes in infrared optical properties. The measurements are closely related to sub-bandgap *photomodulation* measurements, which have been extensively studied in the last twenty years.[5]

In the present work we present measurements of sub-bandgap optical properties in *reverse biased* diodes; injection currents are negligible, and hence the Eggert & Paul mechanism is not applicable directly. We nonetheless find a readily measurable infrared electromodulation band with a prominent maximum near 0.8 eV in several samples. Based primarily on the fact that this band depends linearly upon the electric-field across the device, we attribute it to changes in infrared absorption due to depletion of bandtail states near the interface of the strongly doped, n^+ layer and the intrinsic layer. The linearity of the signal derives from the linear dependence on reverse bias of the space-charge stored near the two interfaces.

This electromodulation band has several interesting features. First, its principal feature at about 0.8 eV is fairly narrow (roughly 0.1 eV), which we believe to be a direct measurement of the width of the D^- (negatively charged dangling bond) band in *n*-type a-Si:H. This electromodulation feature is quite similar to the photoluminescence spectrum for *n*-type a-Si:H. However, we suggest that the optical transition must be internal to a complex involving a D^-, as opposed to one involving an unrelated bandtail level as the final state. We also observe a broader spectral feature at 1.1 eV, which we have not identified.

The second interesting aspect of the sub-bandgap electromodulation effect is that the spectral shape and strength of the band are a diagnostic for the interfaces with doped layers. Indeed the main 0.8 eV feature is absent in a *pin* sample from one laboratory; we compare the spectra for cells with amorphous and microcrystalline n^+ layers from a different laboratory. Finally, we speculate about the linear electromodulation corresponding to interband optical transitions in doped layers; such an effect would complement the true interband electroabsorption effect, which is quadratic in field. Such a linear signal may affect the analysis of electromodulation effects to obtain built-in potentials across a-Si:H based devices. [6,7,8]

Experimental Information

Three different types of sample have been used in the experiments. The first type consisted of Schottky diodes prepared at the Institute of Energy Conversion; the diodes were deposited in the sequence glass/SnO_2/n_+/a-Si:H/TCO. The series included diodes with both microcrystalline and amorphous silicon n_+ layers, and several types of transparent conducting oxide (TCO); the samples used for the present work had indium tin oxide (ITO) TCOs. The diodes had an absorber layer thickness of 0.50 μm and an area of 0.40 cm^2. The second type of sample consisted of *nip* solar cells prepared at United Solar Systems Corp.; these cells were deposited in the sequence stainless-steel/Ag/a-Si:H:P/a-Si:H/μc-Si:H:B/ITO; the Ag back reflector in these cells has a moderate texture to improve The cells had an absorber layer thickness of 0.225 μm and an area of 0.25 cm^2. The third type of sample consisted of *pin* solar cells prepared at Solarex Thin Films Division; these cells were deposited in the sequence glass/SnO_2/a-SiC:H:B/a-Si:H/a-Si:H:P/ITO.

Electromodulation spectra (EA) were measured by applying a sinusoidal bias potential across a sample and measuring the corresponding modulation of the transmission or reflection of an optical beam. The beam itself came from a small illuminator/monochromator with 1 nm resolution. The beam intensity was detected using either a Si or an InGaAs photodetector. We typically used a 10 kHz modulation frequency. We employed a computer to record the electroabsorption spectrum; the spectra reported here are the average of many such spectra taken as rapidly as possible. In general the actual spectrum reported is for the modulation ratio of the optical intensity; the actual amplitude of the modulated detector photocurrent has been divided by the unmodulated photocurrent. This procedure yields a relative modulation spectrum $\delta T/T$ or $\delta R/R$. Some additional details may be found in prior publications from our research group.[3,8,9]

We comment briefly on the modulated reflection spectra on the *nip* solar cells prepared on stainless steel substrates. For longer wavelengths, most of the incident light passes through the top interfaces and propagates to the rear of the sample, where it is reflected by the silver "back reflector." For this reason the "modulated reflection" spectra are sensitive to bulk electroabsorption processes as well as to true "electroreflectance" effects.

Electromodulation Measurements

We first present electromodulated reflectance spectra measured for the *nip* solar cell from United Solar Systems Corp. In the upper panel of Fig. 9 we show these spectra measured for three different values of the modulation field $\delta E = \delta V/d$. The spectrum shows the broad interband electroabsorption peaked near 1.8 eV which has been reported by several previous authors. The electromodulation corresponds to a decrease in reflectance with a decrease in voltage (ie. an increase in reverse bias). There are additional bands near 0.8 and 1.3 eV which are the principal subject of this paper. They are of course almost certainly due to optical transitions involving localized defect states somewhere in the sample. The oscillatory character of the bands near 0.8 eV and 1.3 eV is most likely an artifact of interference fringes; the raw transmission or reflection spectra do show extrema near the zero-crossings for these bands.

Transmittance spectra without these oscillations were obtained using Schottky diode samples, as will be shown shortly.

There is a clear difference in the effects of electric field for the new bands (at 0.8 and 1.3 eV) *vis a vis* the better known band at 1.8 eV. The difference is illustrated in the lower panel of Fig. 9, where we show spectra for varying DC bias across the sample. For this figure the modulation amplitude was held constant. The main band near 1.8 eV, which is generally attributed to electric field effects on the matrix element for valence to conduction band transitions in a-Si:H, is plainly increased by the DC field. This behavior is consistent with the highly accurate quadratic dependence of interband electroabsorption upon electric field amorphous semiconductors.

The band near 0.8 eV in particular shows little dependence upon DC bias voltage; this behavior is consistent with an electromodulation effect that is linear in applied bias voltage. The band at 1.3 eV has a weak dependence upon DC bias voltage, suggesting that it has contributions both from linear and quadratic processes.

In Fig. 10 we present the spectra for two Schottky diode samples from the Institute of Energy Conversion

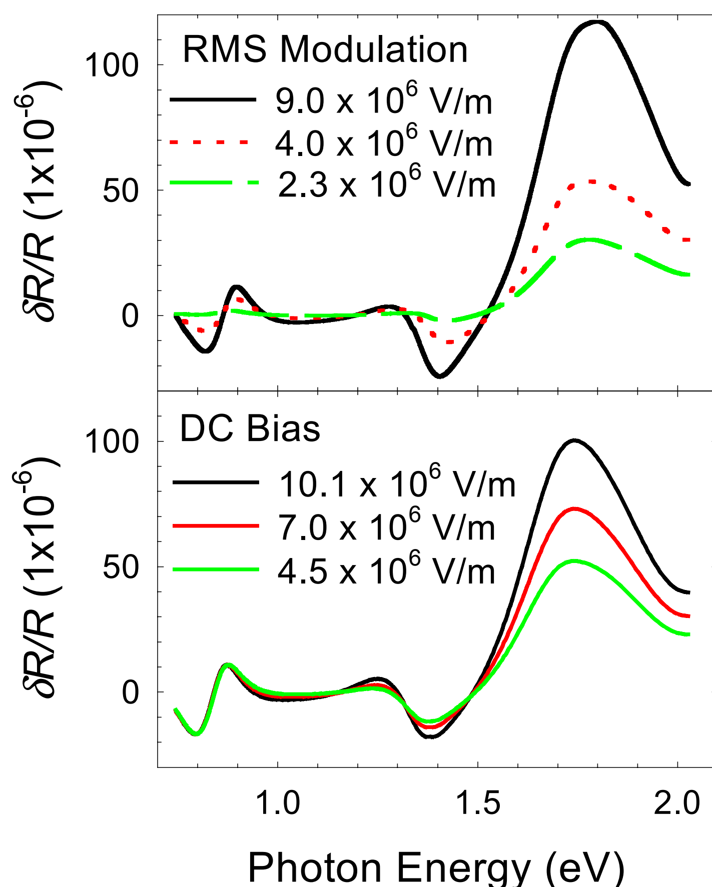

Fig. 9: The two panels show the electromodulated reflection spectra for a-Si:H based *nip* diodes from United Solar Systems Corp. The upper panel illustrates the dependence upon the amplitude of the electric field modulation assuming a uniform field across the undoped intrinsic layer. Both the sub-bandgap and interband electromodulation is essentially linear in electric field. The lower panel illustrates the dependence upon the mean, unmodulated external electric field across the diode; the sub-bandgap electromodulation is independent of the unmodulated field, whereas the interband electromodulation depends linearly upon it.

with varying n^+ materials (a-Si:H and μc-Si:H). Both samples show a peak near 0.8 eV that appears comparable to the oscillating band found near 0.8 eV in the *nip* cell. As in the *nip* solar cells, the EA spectrum peaked near 0.8 eV is almost independent of DC bias voltage: the signal depends linearly upon the bias voltage. Note that the oscillatory behavior for the 0.8 eV band found in the *nip* cells does not appear for the Schottky samples; the absence of interference fringe effects of course simplifies the spectrum enormously. One sees that the two different cells, which have differing n^+ layers, have spectra which differ modestly in spectrum (note the slight shift of the peak near 0.8 eV for the two types of sample) and also in amplitude. In the next section we present a model which accounts for these infrared features in terms of optical transitions in the n^+ layers very near the interface with the intrinsic absorber layer of the cell.

The lowest family of curves is for the *pin* solar cell from Solarex Thin Films Division. The 0.8 eV feature which was prominent in samples from the Institute for Energy Conversion and from United Solar Systems Corp. is not apparent; there is a weaker, broad feature near 1.2 eV with a negative sign. It is worth noting that the spectral shape and the sign of this feature is reminiscent of the Eggert and Paul results obtained with forward bias.

Models for Sub-Bandgap Electromodulation

In this section we discuss the origins of the infrared electromodulation feature near 0.8 eV. There have been an enormous number of reports for defect states with different spectroscopic methods. Without reviewing this entire literature, it is clear that defect states located in the bandgap of amorphous silicon

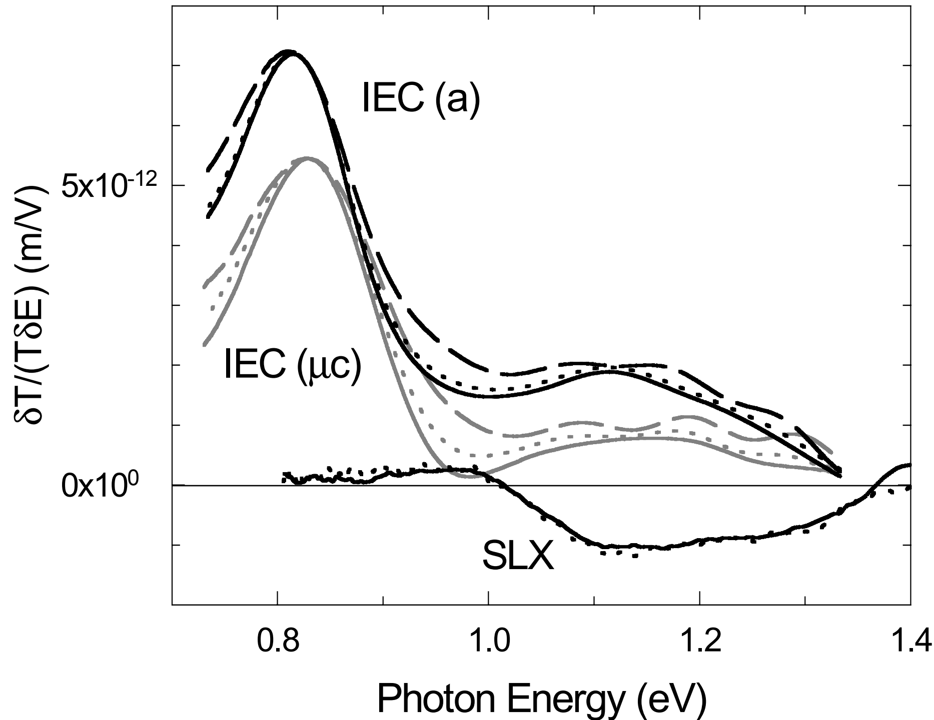

Fig. 10 Normalized electromodulated transmittance *δT/(TδE)* for two Schottky diodes from the Institute of Energy Conversion amorphous silicon {IEC (a)} and microcrystalline silicon {IEC (μ)} n^+ layers, and for one *pin* solar cell from Solarex Thin Films Division (SLX). For each sample results for several DC biases are presented; from the topmost curve of each family the mean fields were (IEC(a) - 1.5, 4.5, and 3.6×10^6 V/m, IEC (μ) - 13.4, 7.6, and 3.6×10^6 V/m, SLX 10.0 and 20.0×10^6 V/m).

thin films are a plausible origin. Nonetheless, we exclude the most obvious identification for these features, which is that they correspond to optical transitions of defects in the relatively thick, intrinsic layer of the cells. Eggert and Paul[4] proposed this identification for electromodulation spectra they measured under forward bias using a Schottky diode. The space-charge of electrons injected into the intrinsic layer under forward bias modifies the occupancy of defects and their associated absorption. Eggert and Paul concluded that their signal corresponded to a *quenching* of the absorption due to the excitation of valence bandtail electrons onto neutral dangling bonds.

Injection of charge into the intrinsic layer is negligible for the reverse-bias conditions in our samples, and we seek a different mechanism than that of Eggert and Paul. We can also exclude the "field-warping" of bandedge states which accounts for interband electroabsorption; although this type of defect electroabsorption no doubt occurs, it would be unlike our measurements. First, the effect should be far weaker than the interband electroabsorption, whereas our infrared electromodulation measurements are only about tenfold weaker than the interband effect. Second, for this mechanism the infrared electromodulation should share the quadratic dependence upon electric-field of the interband process, and our measurements do not.

Although the linear dependence of the 0.8 eV peak on electric field is reminiscent of effects for crystalline solids,[10] the model we favor involves the space charge modulation $C\delta V$ in the n^+ layer by the applied bias; C is the capacitance of the device, which we measured and which was essentially the same as the geometrical capacitance expected if the intrinsic layer were a simple dielectric. Reverse bias reduces the occupancy of states in the conduction bandtail of the n^+ layer. Such depletion will increase the rate at which electrons in relatively deep D^- (or other defect) levels can be optically excited into

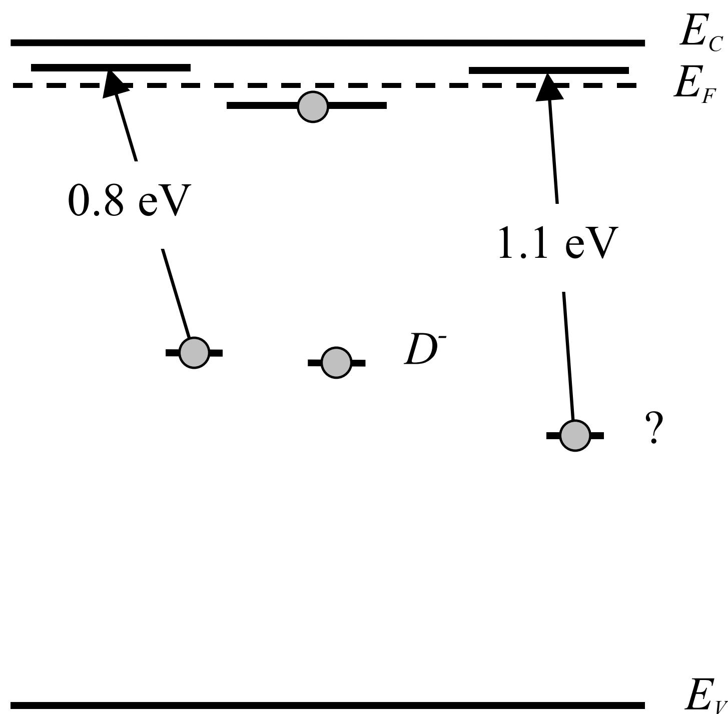

Fig. 11: Schematic illustrating the optical transitions in an n-type a-Si:H layer involved in the model proposed for reverse-bias electromodulation; note in particular the 0.8 eV transition from the well-localized D^- (negatively charged dangling bond) center to a nearby, relatively extended bandtail state, as well as the unidentified 1.1 eV transition.

bandtail states in localized-localized transitions. We illustrate this model in Fig. 3. The 0.8eV transition is the transfer of an electron from a negatively-charged dangling bond D^- to a level located near the Fermi energy of the n^+ material. The model is essentially the inverse of an established model for photoluminescence in strongly *n*-type a-Si:H.[11]

We describe this model using the following expression for the change in transmittance for light passing through the depletion region:

$$\delta T / T = \sigma_{DP} \, C\delta V / e \, ,$$

where σ_{DP} is the cross-section for excitation of an electron from a D^- level to a level just above the Fermi-energy, C is the capacitance per unit area, and δV is the modulation Voltage. A typical value for $C\delta V/e$ is 10^{11} cm^{-2} in our measurements. Typical signals $\delta T/T$ are about 10^{-5}, from which we infer a cross-section of 10^{-16} cm^2. This value appears reasonable.

We next discuss the relative narrowness of the spectrum near 0.8 eV. In the model just described, the final states involved in electromodulation are near the Fermi energy of the n^+ material; they are not spread throughout the conduction band of the material as for most other forms of sub-bandgap spectroscopy. The spectrum should thus reflect the energy-spectrum of D^- levels directly.

We have considered two possible identities for the final state of Fig. 11. The one which is most consistent with prior work on luminescence is to assume that the level is a bandtail state which happens to be close to a D^- level. We exclude this identification using the following argument. If there is significant electromodulation from induced absorption of electrons in D^- levels to otherwise random bandtail states near the Fermi energy, then one should observe a much stronger electromodulation from induced absorption of valence band electrons. Such a strong interband electroabsorption which is linear with applied field is plainly not observed (cf. Fig. 9).

The second identity corresponds to the less conventional assumption that the optical transition in Fig. 3 actually corresponds to an excitation of an intimate, dangling-bond/dopant pair: $D^- P_4^+ + h\nu \rightarrow D^0 P_4^0$. Depletion of electrons from the n^+ layer presumably increases the density of neutral pairs, and reduces the density of negatively charged pairs $D^- P_4^0$. If this identification is accepted, a corresponding modification of models[11] for photoluminescence in *n*-type a-Si:H would also be required: $D^0 P_4^0 \rightarrow D^- P_4^+ + h\nu$ would be the transition corresponding to the 0.8 eV luminescence band. The density-of-states of bandtails in *n*-type a-Si:H certainly includes contributions from dopants as well as intrinsic states, but has not been more quantitatively established.[11,12]

The identification of the 1.1 eV band in Fig. 2 is not clear. We do not think that this feature would have been discernible with better known sub-bandgap spectroscopic techniques such as the constant photocurrent method or photothermal deflection spectroscopy: it is the use of a modulation technique which sharpens the spectra associated with various defects, and permits them to be distinguished. There have been many proposals for other defects in a-Si:H besides the standard triad of *D*-centers, conduction and valence bandtail states. Bond-centered hydrogen and other defects known in crystalline silicon are obvious candidates, but have remained unconfirmed. We cannot exclude that the 1.1 eV band should be associated with one of these.

If we accept the model for the infrared electroabsorption band based on space-charge modulation near the *n/i* interface, then we should be able to use these spectra to help understand this region. In this regard we first note that Eggert and Paul did not find prominent infrared features when they measured electromodulation under reverse bias; we believe that both the weakness of their reverse-bias signal, as well as the absence of the 0.8 eV feature for samples from Solarex, reflects differences between the n^+ materials involved in the various cells. Given these differences, we do find it surprising that the

amorphous and microcrystalline n^+ materials used for preparing the Schottky barrier samples yielded such similar spectra in Fig. 10. The spectra suggest that the actual difference in n^+ material at the *n/i* interface may not be as great as characterizations based on thicker films might suggest.

We chose to neglect the countercharge modulation near the second interface of the intrinsic layer. The neglect is consistent with the observation of similar infrared features for the *nip* solar cells and the Schottky *min* devices, since only the n^+ layers are common elements in the two types of devices. Nonetheless some electroabsorption originating from space-charge modulation of the p^+ layers in *nip* solar cells must also be present. We speculate that the 1.2 eV feature observed with reversed sign in the Solarex *pin* solar cell may be a characteristic of the a-SiC p^+ layers in these cells. We are unable to account for the negative sign of this feature using the relatively simple Fermi-energy modulation model we have described.

References

[1] S. Al Jalali and G. Weiser, J. Non-Crystalline Solids **41**, 1 (1980); G. Weiser, U. Dersch, and P. Thomas, Phil. Mag. **B 57**, 721 (1988).

2 H. Okamoto, K. Hattori, and Y. Hamakawa, *J. Non-Cryst. Solids* **137&138**, 627 (1991) and **164-166**, 893 (1993).

[3] L. Jiang, Q. Wang, E. A. Schiff, S. Guha, and J. Yang, *Appl. Phys. Lett.* **72**, 1060 (1998).

[4] J. R. Eggert and W. Paul, *Phys. Rev. B* **35**, 7993 (1987).

[5] L. Chen, J. Tauc, J.-K. Lee, and E. A. Schiff, *Phys. Rev. B* **43**, 11694 (1991) and references therein.

[6] S. Nonomura, H. Okamoto, and Y. Hamakawa, Jpn. J. Appl. Phys. 21, L464, (1982).

[7] Y. Hamakawa, Semiconductors and Semimetals, Vol **21B**, edited by J. Pankove, p. 141 (1984).

[8] Lin Jiang, Qi Wang, E. A. Schiff, S. Guha, J. Yang, Xunming Deng, *Appl. Phys. Lett.* **69**, 3063 (1996).

[9] Q. Wang, E. A. Schiff, and S. S. Hegedus, in Amorphous Silicon Technology-1994, edited by E. A. Schiff, M. Hack, A. Madan, M. Powell, and A Matsuda (Materials Research Society, Pittsburgh, 1994), Vol. **336**, p. 365.

[10] Y. Yacoby, *Phys. Rev.* **142**, 445 (1966).

[11] R. A. Street, *Hydrogenated Amorphous Silicon* (Cambridge University Press, Cambridge, 1991), p. 130.

[12] H. M. Branz, M. Silver, and D. Adler, *Phil. Mag. B* **57**, 271 (1988).

REPORT DOCUMENTATION PAGE

Form Approved
OMB NO. 0704-0188

Public reporting burden for this collection of information is estimated to average 1 hour per response, including the time for reviewing instructions, searching existing data sources, gathering and maintaining the data needed, and completing and reviewing the collection of information. Send comments regarding this burden estimate or any other aspect of this collection of information, including suggestions for reducing this burden, to Washington Headquarters Services, Directorate for Information Operations and Reports, 1215 Jefferson Davis Highway, Suite 1204, Arlington, VA 22202-4302, and to the Office of Management and Budget, Paperwork Reduction Project (0704-0188), Washington, DC 20503.

1. AGENCY USE ONLY (Leave blank)	2. REPORT DATE December 1999	3. REPORT TYPE AND DATES COVERED Phase I Technical Progress Report, 24 March 1998–23 March 1999

4. TITLE AND SUBTITLE
Electroabsorption and Transport Measurements and Modeling in Amorphous-Silicon-Based Solar Cells; Phase I Technical Progress Report, 24 March 1998–23 March 1999

5. FUNDING NUMBERS
C: XAK-8-17619-23
TA: PV005001

6. AUTHOR(S)
E.A. Schiff, J. Lyou, N. Kopidakis, P. Rao, Q. Yuan

7. PERFORMING ORGANIZATION NAME(S) AND ADDRESS(ES)
Department of Physics
Syracuse University
Syracuse, NY 13244-1130

8. PERFORMING ORGANIZATION REPORT NUMBER

9. SPONSORING/MONITORING AGENCY NAME(S) AND ADDRESS(ES)
National Renewable Energy Laboratory
1617 Cole Blvd.
Golden, CO 80401-3393

10. SPONSORING/MONITORING AGENCY REPORT NUMBER
SR-520-27665

11. SUPPLEMENTARY NOTES
NREL Technical Monitor: B. von Roedern

12a. DISTRIBUTION/AVAILABILITY STATEMENT
National Technical Information Service
U.S. Department of Commerce
5285 Port Royal Road
Springfield, VA 22161

12b. DISTRIBUTION CODE

13. ABSTRACT (Maximum 200 words)
This report describes work done by the Syracuse University during Phase I of this subcontract. Researchers performed work in the following areas:

- In “electroabsorption measurements and built-in potentials in a-Si:H-based solar cells and devices,” researchers obtained an estimate of V_{bi} =1.17 V in cells with a-SiGe:H absorber layers from United Solar Systems Corp.
- In “solar cell modeling employing the AMPS computer program,” researchers began operating a simple “AMPS” modeling site and explored the effect of conduction bandtail width on V_{oc} computed analytical approximations and the AMPS program. The quantitative differences between the two procedures are discussed.
- In “drift mobility measurements in a-Si:H made with high hydrogen dilution,” researchers measured electron and hole mobilities in several *n/i/Ni* (semitransparent) cells from Pennsylvania State University with a-Si absorber layers made under maximal hydrogen dilution and found a modest increase in hole mobility in these materials compared to conventional a-Si:H.
- In “electroabsorption spectroscopy in solar cells,” researchers discovered and interpreted an infrared absorption band near 1.0 eV, which they believe is caused by dopants and defects at the *n/i* interface of cells, and which also has interesting implications for the nature of electroabsorption and for the doping mechanism in *n*-type material.

14. SUBJECT TERMS
photovoltaics ; amorphous silicon ; solar cells ; electroabsorption ; modeling ; AMPS ; transport measurements

15. NUMBER OF PAGES

16. PRICE CODE

17. SECURITY CLASSIFICATION OF REPORT	18. SECURITY CLASSIFICATION OF THIS PAGE	19. SECURITY CLASSIFICATION OF ABSTRACT	20. LIMITATION OF ABSTRACT
Unclassified	Unclassified	Unclassified	UL